

Prediction of narrow N^* and Λ^* resonances with hidden charm above 4 GeV

Jia-Jun Wu^{1,2}, R. Molina^{2,3}, E. Oset^{2,3} and B. S. Zou^{1,3}

1. Institute of High Energy Physics, CAS, Beijing 100049, China

2. Departamento de Física Teórica and IFIC, Centro Mixto Universidad de Valencia-CSIC, Institutos de Investigación de Paterna, Aptdo. 22085, 46071 Valencia, Spain

3. Theoretical Physics Center for Science Facilities, CAS, Beijing 100049, China

(Dated: June 25, 2010)

The interaction between various charmed mesons and charmed baryons are studied within the framework of the coupled channel unitary approach with the local hidden gauge formalism. Several meson-baryon dynamically generated narrow N^* and Λ^* resonances with hidden charm are predicted with mass above 4 GeV and width smaller than 100 MeV. The predicted new resonances definitely cannot be accommodated by quark models with three constituent quarks and can be looked for at the forthcoming PANDA/FAIR experiments.

PACS numbers: 14.20.Gk, 13.30.Eg, 13.75.Jz

Up to now, all established baryons can be ascribed into 3-quark (qqq) configurations [1], although some of them were suggested to be meson-baryon dynamically generated states [2–8] or states with large ($qqqq\bar{q}$) components [9–11]. A difficulty to pin down the nature of these baryon resonances is that the predicted states from various models are around the same energy region and there are always some adjustable ingredients in each model to fit the experimental data. In this letter, we report a study of the interactions between various charmed mesons and charmed baryons within the framework of the coupled channel unitary approach with the local hidden gauge formalism. Several meson-baryon dynamically generated narrow N^* and Λ^* resonances with hidden charm are predicted with mass above 4 GeV and width smaller than 100 MeV. The predicted new resonances can be looked for at the forthcoming PANDA/FAIR experiments [13]. If confirmed, they definitely cannot be accommodated by quark models with three constituent quarks.

We follow the recent approach of Ref. [12] and extend it from three flavors to four. We consider the $PB \rightarrow PB$ and $VB \rightarrow VB$ interaction by exchanging a vector meson, as shown by the Feynman diagrams in Fig. 1.

The effective Lagrangians for the interactions involved are [12]:

$$\begin{aligned}\mathcal{L}_{VVV} &= ig\langle V^\mu[V^\nu, \partial_\mu V_\nu]\rangle \\ \mathcal{L}_{PPV} &= -ig\langle V^\mu[P, \partial_\mu P]\rangle \\ \mathcal{L}_{BBV} &= g(\langle \bar{B}\gamma_\mu[V^\mu, B]\rangle + \langle \bar{B}\gamma_\mu B\rangle\langle V^\mu\rangle)\end{aligned}\quad (1)$$

where P and V stand for pseudoscalar and vector mesons of the 16-plet of $SU(4)$, respectively.

Under the low energy approximation, the three momentum versus the mass of the meson can be neglected. We can just take the γ^0 component of Eq. (1). The three-momentum and energy of the exchanged vector are both much smaller than its mass, so its propagator is approximately $g^{\mu\nu}/M_V^2$. Then with $g = M_V/2f$ the transition potential corresponding to the diagrams of Fig. 1 are

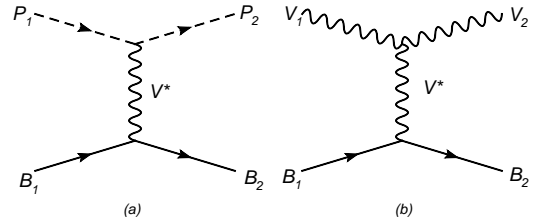


FIG. 1: The Feynman diagrams of pseudoscalar-baryon (a) or vector-baryon (b) interaction via the exchange of a vector meson. P_1, P_2 is D^-, \bar{D}^0 or D_s^-, \bar{D}_s^0 , and V_1, V_2 is D^{*-}, \bar{D}^{*0} or D_s^{*-}, \bar{D}_s^{*0} , and B_1, B_2 is $\Sigma_c, \Lambda_c^+, \Xi_c, \Xi_c'$ or Ω_c , and V^* is ρ, K^*, ϕ or ω .

given by

$$V_{ab(P_1 B_1 \rightarrow P_2 B_2)} = \frac{C_{ab}}{4f^2}(E_{P_1} + E_{P_2}), \quad (2)$$

$$V_{ab(V_1 B_1 \rightarrow V_2 B_2)} = \frac{C_{ab}}{4f^2}(E_{V_1} + E_{V_2})\vec{\epsilon}_1 \cdot \vec{\epsilon}_2, \quad (3)$$

where the a, b stand for different channels of $P_1(V_1)B_1$ and $P_2(V_2)B_2$, respectively. The E is the energy of corresponding particle. The $\vec{\epsilon}$ is the polarization vector of the initial or final vector. And the $\epsilon_{1,2}^0$ component is neglected consistently with taking $\vec{p}/M_V \sim 0$, with \vec{p} the momentum of the vector meson. The C_{ab} coefficients can be obtained by the $SU(4)$ Clebsch Gordan Coefficients which we take from Ref. [14]. We list the values of the C_{ab} coefficients for $PB \rightarrow PB$ with isospin and strangeness $(I, S) = (1/2, 0)$ and $(0, -1)$ explicitly in Table I and Table II, respectively.

With the transition potential, the coupled-channel scattering matrix can be obtained by solving the coupled-channel Bethe-Salpeter equation in the on-shell factorization approach of Refs.[3, 5]

$$T = [1 - VG]^{-1}V \quad (4)$$

with G being the loop function of a meson (P), or a vector (V), and a baryon (B). The poles in the T matrix are

looked for in the complex plane of \sqrt{s} . The $\vec{\epsilon}_1 \cdot \vec{\epsilon}_2$ factor of Eq. (3) factorizes out also in T . Those appearing in the first Riemann sheet below threshold are considered as bound states whereas those located in the second Riemann sheet and above the threshold of some channel are identified as resonances.

TABLE I: Coefficients C_{ab} in Eq. (2) for $(I, S) = (1/2, 0)$

| | | | | | | | | |
|----------------------|-------------------|----------------------|---------------|---------|---------------|-----------|-----------|------------|
| | $\bar{D}\Sigma_c$ | $\bar{D}\Lambda_c^+$ | $\eta_c N$ | πN | ηN | $\eta' N$ | $K\Sigma$ | $K\Lambda$ |
| $\bar{D}\Sigma_c$ | -1 | 0 | $-\sqrt{3}/2$ | -1/2 | $-1/\sqrt{2}$ | 1/2 | 1 | 0 |
| $\bar{D}\Lambda_c^+$ | | 1 | $\sqrt{3}/2$ | -3/2 | $1/\sqrt{2}$ | -1/2 | 0 | 1 |

TABLE II: Coefficients C_{ab} in Eq. (2) for $(I, S) = (0, -1)$

| | | | | | | | | | |
|------------------------|------------------------|----------------|-----------------|-----------------|----------------|---------------|----------------|-------------|--------------|
| | $\bar{D}_s\Lambda_c^+$ | $\bar{D}\Xi_c$ | $\bar{D}\Xi'_c$ | $\eta_c\Lambda$ | $\pi\Sigma$ | $\eta\Lambda$ | $\eta'\Lambda$ | $\bar{K}N$ | $K\Xi$ |
| $\bar{D}_s\Lambda_c^+$ | 0 | $-\sqrt{2}$ | 0 | 1 | 0 | $\sqrt{1/3}$ | $\sqrt{2/3}$ | $-\sqrt{3}$ | 0 |
| $\bar{D}\Xi_c$ | | -1 | 0 | $\sqrt{1/2}$ | $-\frac{3}{2}$ | $\sqrt{1/6}$ | $-\sqrt{1/12}$ | 0 | $\sqrt{3/2}$ |
| $\bar{D}\Xi'_c$ | | | -1 | $-\sqrt{3/2}$ | $\sqrt{3/4}$ | $-\sqrt{1/2}$ | $\frac{1}{2}$ | 0 | $\sqrt{1/2}$ |
| $\eta_c\Lambda$ | | | | 0 | 0 | 0 | 0 | 0 | 0 |

For the G loop function, there are usually two ways to regularize it. In the dimensional regularization scheme one has [5, 12]

$$\begin{aligned}
G &= i2M_B \int \frac{d^4q}{(2\pi)^4} \frac{1}{(P-q)^2 - M_B^2 + i\epsilon} \frac{1}{q^2 - M_P^2 + i\epsilon}, \\
&= \frac{2M_B}{16\pi^2} \left\{ a_\mu + \ln \frac{M_B^2}{\mu^2} + \frac{M_P^2 - M_B^2 + s}{2s} \ln \frac{M_P^2}{M_B^2} \right. \\
&\quad + \frac{\bar{q}}{\sqrt{s}} [\ln(s - (M_B^2 - M_P^2) + 2\bar{q}\sqrt{s}) \\
&\quad + \ln(s + (M_B^2 - M_P^2) + 2\bar{q}\sqrt{s}) \\
&\quad - \ln(-s - (M_B^2 - M_P^2) + 2\bar{q}\sqrt{s}) \\
&\quad \left. - \ln(-s + (M_B^2 - M_P^2) + 2\bar{q}\sqrt{s}) \right\}, \quad (5)
\end{aligned}$$

where q is the four-momentum of the meson, P the total momentum of the meson and the baryon, $s = P^2$ and \bar{q} denotes the three momentum of the meson or baryon in the center of mass frame. μ is a regularization scale, which we take to be 1000 MeV here. Changes in the scale are reabsorbed in the subtraction constant a_μ to make results scale independent.

The second way for regularization is by putting a cutoff in the three-momentum. The formula is [3]:

$$G = \int_0^\Lambda \frac{\bar{q}^2 d\bar{q}}{4\pi^2} \frac{2M_B(\omega_P + \omega_B)}{\omega_P \omega_B (s - (\omega_P + \omega_B)^2 + i\epsilon)} \quad (6)$$

where $\omega_P = \sqrt{\bar{q}^2 + M_P^2}$, $\omega_B = \sqrt{\bar{q}^2 + M_B^2}$, and Λ is the cutoff parameter in the three-momentum of the function loop.

For these two types of G function, the free parameters are a_μ in Eq. (5) and Λ in Eq. (6). We choose a_μ or Λ so that the shapes of these two functions are almost

the same close to threshold and they take the same value at threshold. This limits the a_μ to be around -2.3 with the corresponding Λ around 0.8 GeV, values which are within the natural range for effective theories [5]. Since varying the G function in a reasonable range does not influence our conclusion qualitatively, we present our numerical results in the dimensional regularization scheme with $a_\mu = -2.3$ in this letter.

From the T matrix for the $PB \rightarrow PB$ and $VB \rightarrow VB$ coupled-channel systems, we can find the pole positions z_R . Six poles are found in the real axes below threshold and therefore they are bound states. For these cases the coupling constants are obtained from the amplitudes in the real axis. These amplitudes behave close to the pole as:

$$T_{ab} = \frac{g_a g_b}{\sqrt{s} - z_R}. \quad (7)$$

We can use the residue of T_{aa} to determine the value of g_a , except for a global phase. Then, the other couplings are derived from

$$g_b = \lim_{\sqrt{s} \rightarrow z_R} \left(\frac{g_a T_{ab}}{T_{aa}} \right). \quad (8)$$

The obtained pole positions z_R and coupling constants g_α are listed in Tables III and IV. Among six states, four of them couple only to one channel while two states couple to two channels.

| (I, S) | z_R (MeV) | g_a | | |
|----------|-------------|------------------------|----------------------|-----------------|
| (1/2, 0) | | $\bar{D}\Sigma_c$ | $\bar{D}\Lambda_c^+$ | |
| | 4269 | 2.85 | 0 | |
| (0, -1) | | $\bar{D}_s\Lambda_c^+$ | $\bar{D}\Xi_c$ | $\bar{D}\Xi'_c$ |
| | 4213 | 1.37 | 3.25 | 0 |
| | 4403 | 0 | 0 | 2.64 |

TABLE III: Pole positions z_R and coupling constants g_a for the states from $PB \rightarrow PB$.

| (I, S) | z_R (MeV) | g_a | | |
|----------|-------------|--------------------------|------------------------|-------------------|
| (1/2, 0) | | $\bar{D}^*\Sigma_c$ | $\bar{D}^*\Lambda_c^+$ | |
| | 4418 | 2.75 | 0 | |
| (0, -1) | | $\bar{D}_s^*\Lambda_c^+$ | $\bar{D}^*\Xi_c$ | $\bar{D}^*\Xi'_c$ |
| | 4370 | 1.23 | 3.14 | 0 |
| | 4550 | 0 | 0 | 2.53 |

TABLE IV: Pole position and coupling constants for the bound states from $VB \rightarrow VB$.

As all the states that we find have zero width, we should take into account some decay mechanisms. Thus, we consider the decay of the states to a light baryon plus either a light meson or a charmonium through heavy charmed meson exchanges by means of box diagrams as it was done in [15, 16]. Coupling to these additional channels with thresholds lower than the masses of previously obtained bound states provides decay widths to

these states and modifies the masses of these states only slightly. The results are given in Tables V and VI. We do not consider the transitions between VB and PB states because in our t-channel vector meson exchange model they involve an anomalous VVP vertex which is found to be very small [15]. The transitions between VB and PB states through t-channel pseudoscalar meson exchanges are also found to be very small. As an example, we estimate the partial decay width of our $\bar{D}\Sigma_c$ molecular state $N_{c\bar{c}}^{*+}(4265)$ to the $J/\psi p$ final state through the t-channel pseudoscalar D^0 meson exchange as shown by Fig. 2. Following a similar approach as in Ref. [17], the partial decay width is about 0.01 MeV, which is 3 orders of magnitude smaller than the corresponding decay to $\eta_c p$ of 23.4 MeV.

| (I, S) | M | Γ | Γ_i | | | | | |
|------------|------|----------|------------|-------------|---------------|----------------|------------|-----------------|
| $(1/2, 0)$ | 4261 | 56.9 | πN | ηN | $\eta' N$ | $K\Sigma$ | $\eta_c N$ | |
| | | | 3.8 | 8.1 | 3.9 | 17.0 | 23.4 | |
| $(0, -1)$ | 4209 | 32.4 | $K N$ | $\pi\Sigma$ | $\eta\Lambda$ | $\eta'\Lambda$ | $K\Xi$ | $\eta_c\Lambda$ |
| | | | 15.8 | 2.9 | 3.2 | 1.7 | 2.4 | 5.8 |
| | | | 4394 | 43.3 | 0 | 10.6 | 7.1 | 3.3 |

TABLE V: Mass (M), total width (Γ), and the partial decay width (Γ_i) for the states from $PB \rightarrow PB$, with units in MeV.

| (I, S) | M | Γ | Γ_i | | | | | |
|------------|------|----------|------------|--------------|-----------------|---------------|----------|-----------------|
| $(1/2, 0)$ | 4412 | 47.3 | ρN | ωN | $K^*\Sigma$ | $J/\psi N$ | | |
| | | | 3.2 | 10.4 | 13.7 | 19.2 | | |
| $(0, -1)$ | 4368 | 28.0 | $K^* N$ | $\rho\Sigma$ | $\omega\Lambda$ | $\phi\Lambda$ | $K^*\Xi$ | $J/\psi\Lambda$ |
| | | | 13.9 | 3.1 | 0.3 | 4.0 | 1.8 | 5.4 |
| | | | 4544 | 36.6 | 0 | 8.8 | 9.1 | 0 |

TABLE VI: Mass (M), total width (Γ), and the partial decay width (Γ_i) for the states from $VB \rightarrow VB$ with units in MeV.

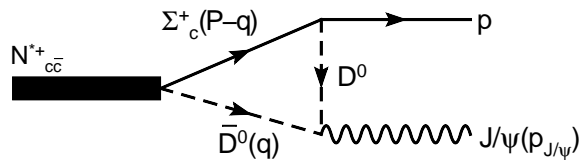


FIG. 2: Feynman diagram for $N_{c\bar{c}}^{*+}(4265) \rightarrow J/\psi p$.

It is very interesting that the six N^* and Λ^* states are all above 4200 MeV, but with quite small decay widths. In principle, one might think that the width of these massive objects should be large because there are many channels open and there is much phase space for decay. However, because the hidden $c\bar{c}$ components involved in these states, all decays within our model are tied to the necessity of the exchange of a heavy charmed vector meson and hence are suppressed. If these predicted narrow N^* and Λ^* resonances with hidden charm are found, they definitely cannot be accommodated by quark models with three constituent quarks.

In order to look for these predicted new N^* and Λ^* states, we estimate the production cross section of these resonances at FAIR. With a \bar{p} beam of 15 GeV/c one has $\sqrt{s} = 5470$ MeV, which allows one to observe N^* resonances in $\bar{p}X$ production up to a mass $M_X \simeq 4538$ MeV or Y^* hyperon resonances in $\bar{\Lambda}Y$ production up to a mass $M_Y \simeq 4355$ MeV. We take $N_{c\bar{c}}^{*+}(4265)$ as an example. Its largest decay channel is $\eta_c p$. Following the approach as in Ref. [18], we calculate its contribution to $p\bar{p} \rightarrow p\bar{p}\eta_c$ through processes as shown in Fig. 3(a,b) and also those from the conventional mechanism as shown in Fig. 3(c,d). For the conventional mechanism, the $pp\eta_c$ coupling is determined from the partial decay width of $\eta_c \rightarrow p\bar{p}$ [1]. For the new mechanism with the $N_{c\bar{c}}^{*+}(4265)$, its couplings to $\eta_c p$ and πp are determined from its corresponding partial decay widths listed in Table V. It is found that while the conventional mechanism gives a cross section about $0.1nb$, the new mechanism with the $N_{c\bar{c}}^{*+}(4265)$ results in a cross section about $0.1\mu b$, about 3 orders of magnitude larger. With the designed luminosity of about $10^{31}cm^{-2}s^{-1}$ for the \bar{p} beam at FAIR [13], this corresponds to an event production rate of more than 80000 per day. With branching ratios for $\eta_c \rightarrow K\bar{K}\pi, \eta\pi\pi, K^+K^-\pi^+\pi^-, 2\pi^+2\pi^-$ of a few percent for each channel, the $N_{c\bar{c}}^{*+}(4265)$ should be easily observed from the $\eta_c p$ and $\eta_c\bar{p}$ invariant mass spectra for the $p\bar{p} \rightarrow p\bar{p}\eta_c$ reaction by the designed PANDA detector [13]. The $N_{c\bar{c}}^{*+}(4265)$ should also be easily observed in the $p\bar{p} \rightarrow p\bar{p}J/\psi$ reaction with clean J/ψ signal from its large decay ratio to e^+e^- and $\mu^+\mu^-$ although the production rate is about 3 orders of magnitude smaller than the $p\bar{p} \rightarrow p\bar{p}\eta_c$ process.

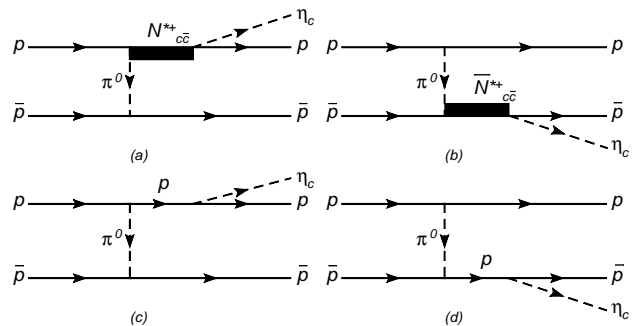


FIG. 3: Feynman diagrams of the reaction $p\bar{p} \rightarrow p\bar{p}\eta_c$

The $\bar{D}^*\Sigma_c$ molecular state $N^*(4415)$ has a large decay branching ratio to $J/\psi p$. Its contribution to the $p\bar{p} \rightarrow p\bar{p}J/\psi$ reaction is estimated to be around $2nb$, about one order of magnitude larger than the contribution from the $N_{c\bar{c}}^{*+}(4265)$, and hence should be observed more clearly in this reaction. Similarly, the predicted $D_s^-\Lambda_c^+-\bar{D}\Xi_c$ coupled-channel bound state $\Lambda_{c\bar{c}}^*(4210)$ states should be easily observed in $p\bar{p} \rightarrow \Lambda\bar{\Lambda}\eta_c$ reaction at FAIR. The other three predicted $\Lambda_{c\bar{c}}^*$ resonances have too high

masses to be produced at FAIR, but may be studied in some future facilities with higher \bar{p} beam energies by the $p\bar{p} \rightarrow \Lambda\bar{\Lambda}\eta_c$ or $p\bar{p} \rightarrow \Lambda\bar{\Lambda}J/\psi$ reactions. This is an advantage for their experimental searches, compared with those baryons with hidden charms below $\eta_c N$ threshold proposed by other approaches [19].

In summary, we find two $N_{c\bar{c}}^*$ states and four $\Lambda_{c\bar{c}}^*$ states from PB and VB channels by using the local hidden gauge Lagrangian in combination with unitary techniques in coupled channels. All of these states have large $c\bar{c}$ components, so their masses are all larger than 4200 MeV. The width of these states decaying to light meson and baryon channels without $c\bar{c}$ components are all very small. On the other hand, the $c\bar{c}$ meson - light baryon channels are also considered to contribute to the width to these states. Then $\eta_c N$ and $\eta_c \Lambda$ are added to the PB channels, while $J/\psi N$ and $J/\psi \Lambda$ are added in the VB channels. The widths to these channels are not negligible, in spite of the small phase space for the decay, because the exchange D^* or D_s^* mesons were less off-shell than the corresponding one in the decay to light meson - light baryon channels. The total width of these states are still very small. We made some estimates of cross sections for production of these resonances at the upcoming FAIR facility. The cross section of the reaction $p\bar{p} \rightarrow p\bar{p}\eta_c$ and $p\bar{p} \rightarrow p\bar{p}J/\psi$ are about $0.1\mu b$ and $0.2nb$, in which the main contribution comes from the predicted $N_{c\bar{c}}^*(4265)$ and $N_{c\bar{c}}^*(4415)$ states, respectively. With this theoretical results, one can estimate over 80000 and 1700 events per day at the PANDA/FAIR facility. Similar event rate is expected for the predicted $\Lambda_{c\bar{c}}^*(4210)$ state in the $p\bar{p} \rightarrow \Lambda\bar{\Lambda}\eta_c$ reaction. These 3 predicted new narrow N^* and Λ^* resonances should be easily observed by the PANDA/FAIR. The other 3 predicted $\Lambda_{c\bar{c}}^*$ resonances will remain for other future facilities to discover.

Although in the scheme of dynamical generated states these new $N_{c\bar{c}}^*$ and $\Lambda_{c\bar{c}}^*$ states are simply brothers or sisters of the well-known $N^*(1535)$ and $\Lambda^*(1405)$ in the hidden charm sector, their discovery will be extremely important. While for the $N^*(1535)$, $\Lambda^*(1405)$ and many other proposed dynamical generated states cannot clearly distinguish them from those generated states in various quenched quark models with qqq for baryon states and $q\bar{q}$ for meson states due to many tunable model ingredients, these new narrow N^* and Λ^* resonances with mass above 4.2 GeV definitely cannot be accommodated by the conventional 3q quark models, although how to distinguish these meson-baryon dynamically generated states from possible five-quark states needs more detailed scrutiny. The existence of these new resonances with hidden charm may also have important implications to the long-standing puzzles relevant to charmonium production in various collisions involving nucleon in the initial state, such as the strikingly large spin-spin correlation observed in pp elastic scattering near charm production threshold [20] and difficulties in reproducing the cross

sections and polarization observables of J/ψ production from high energy $\bar{p}p$, pp and γp reactions [21, 22]. These issues deserve further exploration.

We thank Li-sheng Geng and Feng-kun Guo for useful discussions. This work is partly supported by DGI-CYT Contract No. FIS2006-03438, the Generalitat Valenciana in the project PROMETEO and the EU Integrated Infrastructure Initiative Hadron Physics Project under contract RII3-CT-2004-506078. This work is also partly supported by the National Natural Science Foundation of China (NSFC) under grants Nos. 10875133, 10821063, and by the Chinese Academy of Sciences under project No. KJCX3-SYW-N2, and by the Ministry of Science and Technology of China (2009CB825200).

-
- [1] Particle Data Group, C. Amsler *et al.*, Phys. Lett. B **667**, 1 (2008).
 - [2] N. Kaiser, P. B. Siegel and W. Weise, Phys. Lett. B **362**, 23 (1995).
 - [3] E. Oset and A. Ramos, Nucl. Phys. A **635**, 99 (1998).
 - [4] J. A. Oller, E. Oset and A. Ramos, Prog. Part. Nucl. Phys. **45**, 157 (2000).
 - [5] J. A. Oller and U. G. Meissner, Phys. Lett. B **500**, 263 (2001).
 - [6] T. Inoue, E. Oset and M. J. Vicente Vacas, Phys. Rev. C **65**, 035204 (2002)
 - [7] C. Garcia-Recio, M. F. M. Lutz and J. Nieves, Phys. Lett. B **582**, 49 (2004).
 - [8] T. Hyodo, S. I. Nam, D. Jido and A. Hosaka, Phys. Rev. C **68**, 018201 (2003)
 - [9] C. Helminen and D. O. Riska, Nucl. Phys. A **699**, 624 (2002).
 - [10] B. C. Liu, B. S. Zou, Phys. Rev. Lett. **96**, 042002 (2006); *ibid.*, **98**, 039102 (2007).
 - [11] B. S. Zou, Nucl. Phys. A **835**, 199 (2010).
 - [12] E. Oset and A. Ramos, Euro. Phys. J. A **44**, 445 (2010).
 - [13] M. F. M. Lutz et al. [The PANDA Collaboration], arXiv:0903.3905 [hep-ex].
 - [14] E. M. Haacke, J. W. Moffat and P. Savaria, J. Math. Phys. **17**, 2041 (1976).
 - [15] R. Molina, D. Nicmorus and E. Oset, Phys. Rev. D **78**, 114018 (2008)
 - [16] L. S. Geng and E. Oset, Phys. Rev. D **79**, 074009 (2009)
 - [17] R. Molina, D. Gamermann, E. Oset and L. Tolos, Eur. Phys. J. A **42**, 31 (2009)
 - [18] J. J. Wu, Z. Ouyang and B. S. Zou, Phys. Rev. C **80**, 045211 (2009).
 - [19] S. J. Brodsky, I. A. Schmidt and G. F. de Teramond, Phys. Rev. Lett. **64**, 1011 (1990); C. Gobbi, D. O. Riska and N. N. Scoccola, Phys. Lett. B **296**, 166 (1992); J. Hofmann and M. F. M. Lutz, Nucl. Phys. A **763**, 90 (2005).
 - [20] S. J. Brodsky and G. F. de Teramond, Phys. Rev. Lett. **60**, 1924 (1988).
 - [21] N. Brambilla *et al.* [Quarkonium Working Group], arXiv:hep-ph/0412158, and references therein.
 - [22] B. Gong, X. Q. Li and J. X. Wang, Phys. Lett. B **673**, 197 (2009).